

The Observation of Ionospheric Large-Scale Wave Structure In Southeast Asia

Liow Yu-Yi¹, Suhaila M Buhari², Mardina Abdullah³, Tajul Ariffin Musa⁴, Tulasiram Sundarsanam⁵

¹Physics Department, Universiti Teknologi Malaysia, Johor Bahru, Malaysia

²Scientific Computational Research Group, Universiti Teknologi Malaysia, Johor Bahru, Malaysia

³Space Science Center, Univeristi Kebangsaan Malaysia, Bangi, Malaysia

⁴Geomatic Innovation Research Group, Univeristi Teknologi Malaysia, Johor Bahru, Malaysia

⁵Indian Institute of Geomagnetism, Mumbai, India

liowyuyi@hotmail.com, suhailamb@utm.my, mardina@eng.ukm.my, tajulariffin@utm.my, s.tulasiram@gmail.com

Abstract—The occurrence of the equatorial plasma bubble (EPB) at nighttime always leads to the scintillation and fluctuation of radio wave signals from satellites. The observation in the seeding perturbation of EPB is important to understand the seeding mechanism of EPB. In this paper, a large-scale wave structure (LSWS) formed at the bottom side of the F layer is studied using GNU Radio Beacon Receiver (GRBR) that receives data from Communications/Navigation Outage Forecasting System (C/NOFS). The LSWS was determined from the high variations of total electron content (TEC) along the path of C/NOFS to GRBR. The study shows that LSWS component was developed around the E-region sunset (SSE) for both days on December 2012 and April 2013 and only the day from April 2013 showed the presence of nighttime EPBs after the development of LSWS. The results show that the LSWS may be present during the late evening with no occurrence of EPB in the post-sunset. However, the results can be verified by investigating more beacon data and the minimum amplitude of LSWS to develop EPBs.

Keywords—large-scale wave structure; equatorial plasma bubble; ionospheric irregularities; C/NOFS.

I. INTRODUCTION

Communication satellite system is used extensively in civilian and military purpose in daily life in the modern society. The signals of the satellite transmitted from the space medium and to the receivers at the surface earth. The accuracy and precision of the transmitted signals are greatly affected by the activities that occurred in space medium that is constantly under the exposure of radiation, geomagnetic storm and so on. The conditions of the space medium, especially the ionospheric activities in atmosphere have been observed and studied using the Global Satellite Navigation System (GNSS) [1]. This is important in improving the accuracy of the signal transmission of satellites from the space medium to the earth for both civilian and military use by understanding the mechanism and properties of the ionosphere. Equatorial plasma bubble (EPB) or equatorial spread F (ESF) are known as the ionospheric irregularities that occurred during the post sunset time and signals will be greatly affected due to the change in electron density in ionosphere.

It is believed that the seed perturbation for the formation of EPB might be the atmospheric gravity wave (AGW) and large-scale wave structure (LSWS) [2, 3, 4]. AGW developed in the lower part atmosphere in stratosphere and then travelled upwards to the thermosphere. The upward motion of AGW

results in the perturbation at the bottom surface of the F layer causing the increase in the growth rate of Rayleigh-Taylor instability (RTI) [4, 5, 6]. RTI is a phenomenon where a denser fluid located above a less dense fluid. The high RTI may lead to the development of a quasiperiodic structure which is known as LSWS at the bottom side of the F layer during the post sunset rise (PSSR) [3, 7]. EPB is then formed from the crest of the upwellings or LSWS. However, the seeding mechanism of EPB is still yet to be fully understood due to the lack of observation in seeding perturbation of the EPB.

Many studies have been carried out to observe the development of LSWS. LSWS component at the bottomside of F layer was observed using ALTAIR radar in early time and it was found that the occurrence of EPBs highly related to LSWS [3, 8]. As reported by Tsunoda 2005, the occurrence of EPBs are due to the presence of LSWS in the bottomside of F layer [8]. The first observation of LSWS by using Coherent Electromagnetic Radio Tomography (CERTO) radio beacon on-board Communications/Navigation Outage Forecasting System (C/NOFS) was made by Thampi et al in 2009 [9]. The low inclination satellites like C/NOFS allow one to detect the LSWS component at the subsurface of F layer near the equatorial region. The study of relationship between LSWS component and EPBs in both Asia and African region shows that the LSWS component developed around the local sunset time and the component can be found just before the E-region sunset (SSE) [4, 8, 9]. Its results also indicate the alignment of the LSWS and the geomagnetic field around SSE [4]. The occurrence of EPBs are observed when higher amplitude of LSWS are developed [4].

In this paper, two days data from solstice month, December and near equinox month, April are chosen to study the relationship between LSWS and EPBs and comparison between these two days are made, i.e. the day with and without occurrence of EPBs. The signature of EPB or the LSWS at the bottom side of F layer is studied by using low earth orbiting satellites (LEOS). C/NOFS beacon data is chosen as its satellite altitude as low as 500 km. The properties of the LSWS are investigated.

II. OBSERVATION AND DATA

GRBR was used in investigating the LSWS as the properties of LSWS at the subsurface of F layer are unable to detect using the Global Positioning System (GPS) due to its high altitude. GRBR developed by Yamamoto [10] was used to observe the properties of the LSWS in the late evening. It is used to estimate the total electron content (TEC) of the ionosphere especially the subsurface of F layer. C/NOFS beacon data received from GRBR installed in Kuala Lumpur, Malaysia is chosen in this study. Fig. 1 shows the location of GRBR in Kuala Lumpur.

GRBR operates based on the frequencies of radio signal at 150 MHz and 400 MHz. The propagation of radio wave in the ionosphere with its refractive index, n is

$$u = U \cos [2\pi f (nx/c - t)] \quad (1)$$

where U is signal amplitude, f is signal frequency, x is position, c is speed of light, and t is time. At higher frequency, the refractive index, n is explained by the frequency function and the free electron density, N as

$$n = 1 - (AN/2f^2) \quad (2)$$

where $A = [e^2/(2\pi)^2 m \epsilon_0] = 80.6 \text{ m}^3/\text{s}^2$, and the permittivity of free space, $\epsilon_0 = 8.854 \times 10^{-12} \text{ F/m}$, e is the electron charge, and m is the mass of electron. The total phase, Ψ at travel length, L is expressed as

$$\Psi = (2\pi f/c)L - \pi A/cf \int N dx + \eta \quad (3)$$

where $\int N dx$ is total electron content, η is the unknown constant of phase bias of system. L is then eliminated by taking two radio waves f_1 and f_2 where $f_1 = pf$ and $f_2 = qf$. Taking $f_1 = 150 \text{ MHz}$, $f_2 = 400 \text{ MHz}$, $p = 3$, and $q = 8$, the difference between Ψ_1 and Ψ_2 , ϕ yields

$$\phi = \Psi_1/p - \Psi_2/q = (\pi A/f_1 c)(1/q^2 - 1/p^2) \int N dx + \eta'. \quad (4)$$

The path difference between two frequencies is known as the TEC of ionosphere. To observe LSWS in TEC units, TEC in zonal distance must be subtracted from the running average of 2.5 min of TEC.

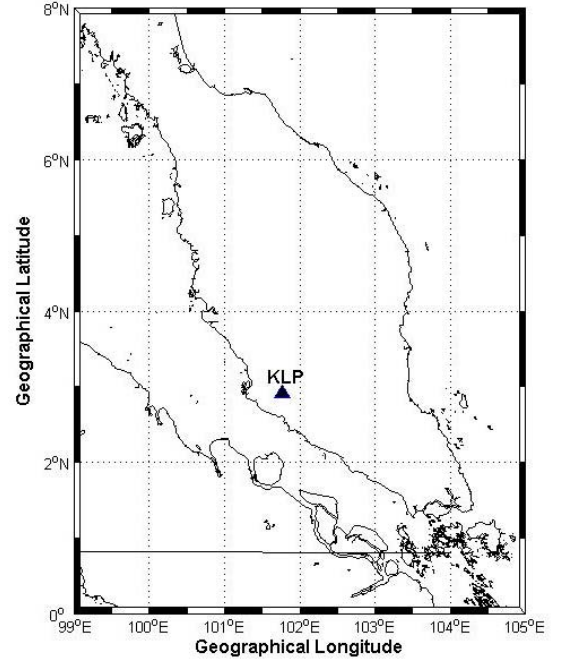


Fig. 1. Location of GRBR in Kuala Lumpur, Malaysia.

K_p index was obtained from Data Analysis Centre for Geomagnetism and Space Magnetism, Kyoto (<http://wdc.kugi.kyoto-u.ac.jp/kp/>) and solar flux index $F_{10.7}$ is obtained from OMNIWeb (<http://omniweb.gsfc.nasa.gov/form/dx1.html>).

Table 1 shows the K_p index and solar flux index $F_{10.7}$ in both 20 Dec 2012 and 4 April 2013. Both of the day showed high solar flux index that exceeded 100 and K_p index less than 4. As reported by Buhari et al. 2017, there will be high chance of occurrence of EPB during the high solar flux activity and there is no significant effect of geomagnetic conditions on the occurrence of EPB [11].

TABLE I. SOLAR ACTIVITY AND GEOMAGNETIC CONDITION

| Date | K_p Index | $F_{10.7}$ cm |
|--------------|-------------|---------------|
| 20 Dec 2012 | 3 | 110.4 |
| 4 April 2013 | 2 | 128.6 |

III. RESULTS AND DISCUSSIONS

LSWS in TEC units on 20 Dec 2012 was calculated from 0813 UT to 1320 UT for four successive orbits. Fig. 2 plotted the graph of LSWS versus longitude of ionospheric piercing point (IPP) for GRBR in Kuala Lumpur. One can observe the amplitude of LSWS does not vary much around 0813 UT and 0955 UT. The green dotted and red dotted lines represent the E region sunset and F region sunset. A higher depletion of LSWS can be seen around 1137 UT orbit, represents by yellow shades between 100°E - 110°E longitudes. The yellow shades were extended to the previous orbit shows that the higher depletion of

LSWS around orbit 1137 UT may associated with small variations of LSWS around orbit 0955 UT. The results may infer that the LSWS can be observed using GRBR in the early evening hour [6]. However, the next pass of C/NOFS satellite in 1320 UT observed no development of EPB although the higher depletion of LSWS component is formed in 1137 UT. The results indicate that existence of LSWS in the late evening may not necessarily lead the formation of EPBs in the post sunset hour. This is consistent with previous study that 30% of LSWS events were not followed by the occurrence of EPB particularly during solstice months [12]. Furthermore, the data in Fig.2 was taken during solstice month which is not a favorable season for EPB formation.

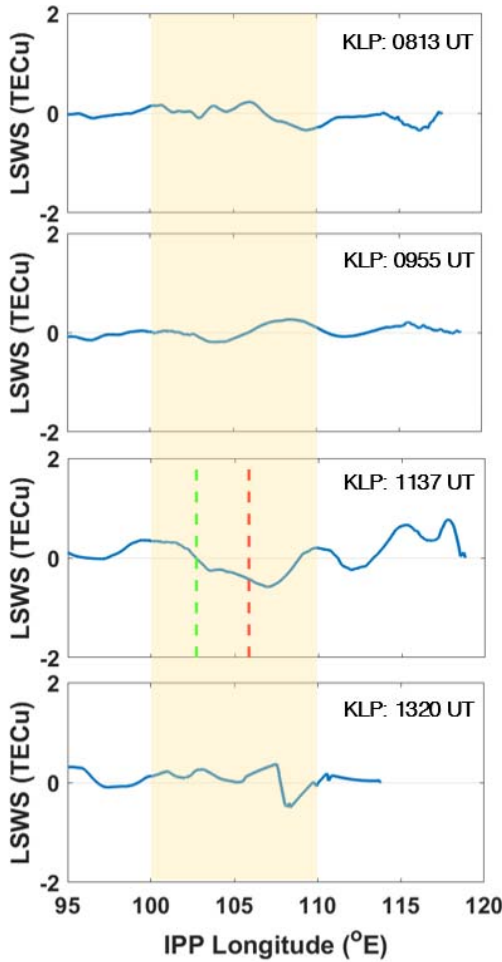


Fig. 2. LSWS in TEC units on 20 Dec 2012.

Scintillation for both signals were plotted for orbit 1137 UT which exhibits high amplitude of LSWS depletion. The red and blue color represents the scintillation for 150MHz and 400MHz as shown in Fig. 3. No scintillations were observed along the longitude indicated that no EPB was formed and can be considered as LSWS component [4].

LSWS in TEC units on 4 April 2013 was calculated from 0813 UT to 1320 UT for four successive orbits as shown in Fig.

4. The first and second C/NOFS pass around 0813 UT and 0955 UT show small depletions of LSWS around 96°E 108°E. Both depletions are marked with red arrows. Large depletion of LSWS up to 1 TECU can be seen during the orbit 1137 UT around 115°E, after the F-region sunset. No scintillations were observed till ~115°E in Fig. 5. The scintillation indicated the present of EPB [4]. The next pass of C/NOFS recorded the larger depletions of LSWS nearly 2 TECU. This showed that the nighttime EPBs formed during the sunset time [1, 4, 8, 11, 13]. However, no data was recorded after the C/NOFS pass to the eastern side of 105°E.

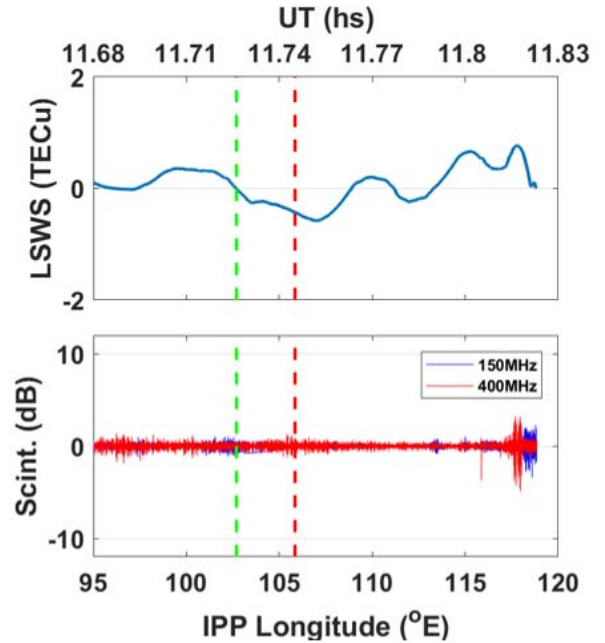


Fig. 3. LSWS and scintillation of signal on 20 Dec 2012.

For both selected data on 20 Dec 2012 and 4 April 2013, the development of LSWS formed around 1130 UT and the LSWS component is nearly zero before 1130 UT. However, formation of EPB only found on the day of 4 April 2013 at 1320 UT. As reported by Tulasi Ram et al. [4], the presence of EPBs on the nighttime were associated to the high amplitude of LSWS component. The amplitude of the LSWS on 4 April 2013 at 1137 UT reached more than 1 TEC units and EPBs were observed in at 1320 UT. This indicates that the high growth of LSWS component as the seed to generate EPBs [4]. Furthermore, the event on 4 April 2013 is during equinox month where the solar terminator is aligned with geomagnetic field. Small amplitude of LSWS in the late evening may lead the development of EPB in the post-sunset hour [11]. Although LSWS is presence during the late evening on the 20 Dec 2013, the amplitude may not enough to seed the EPB during solstice month.

It is believed that the development of LSWS component is AGW from convective activity of the troposphere propagates up to the lower region of thermosphere could cause the growth of LSWS around SSE [3, 14]. No LSWS component is observed during the day time due to the high field line integrated Pedersen conductivity in E layer. The electrical loading in E region started

to reduce around the sunset time and the seeding will occur as shown in Fig. 1 and 2 [4, 14]. The occurrence of EPBs is higher around the equinoxes due to the alignment of solar terminator with magnetic field and lower around the solstices [11, 15, 16]. This is because of the E-region conductivity gradient is the largest during the alignment [15]. The solar flux index of 20 Dec 2012 and 4 April 2013 are 110.4 and 128.6 respectively. It is found that the occurrence of EPB is higher in equinox months during the time with high solar activity due to the high RTI growth rate [11]. The growth of EPBs can be found as early as late afternoon in the crest of upwellings of LSWS and then amplified during the PSSR.

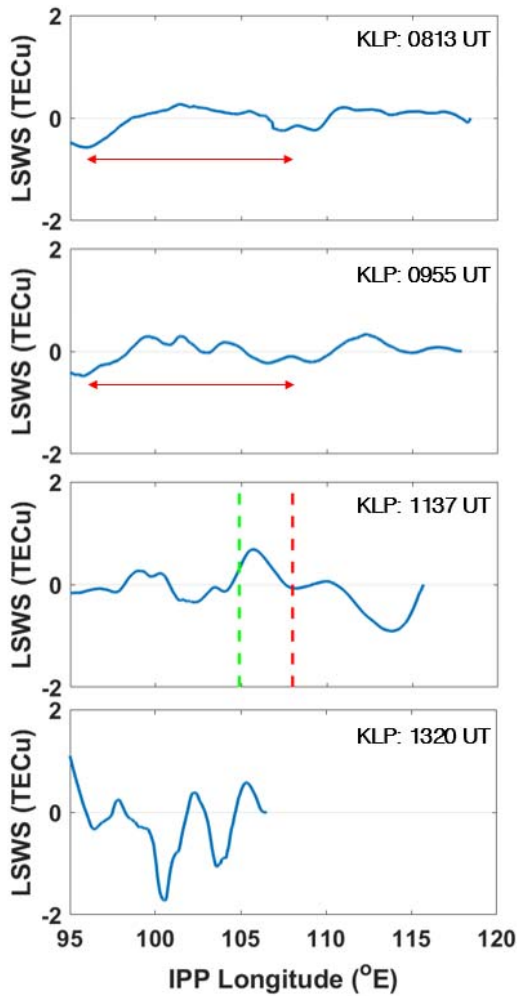


Fig. 4. LSWS in TEC units on 4 April 2013.

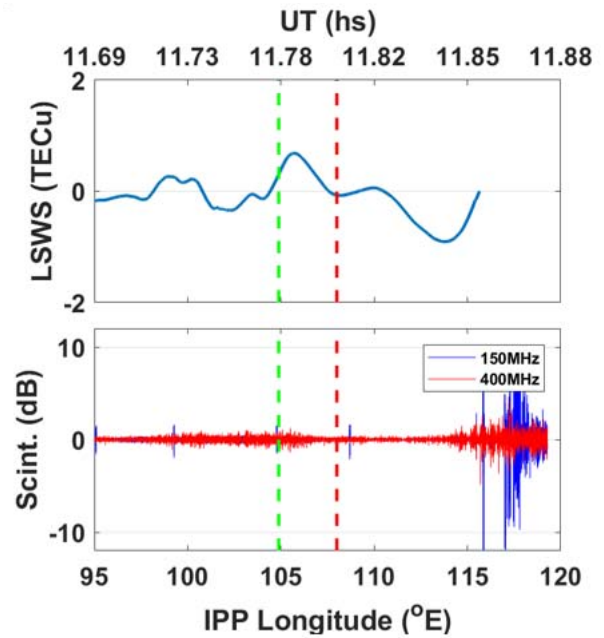


Fig. 5. LSWS and scintillation of signal on 4 April 2013.

IV. CONCLUSION

The LSWS component from the observation of C/NOFS has been successfully calculated and plotted in the graph of LSWS versus IPP longitude. The results showed that LSWS component formed during the late afternoon or SSE for both days in December and April. However, the presence of LSWS does not necessary lead to the growth of EPBs, i.e. no EPBs were formed on 20 December 2012. EPBs occurrence is higher around the equinoxes [15]. For future research, more beacon data are needed to verify the results and the minimum amplitude of LSWS component that required for the growth of EPBs should be identified.

ACKNOWLEDGMENT

The GRBR system was developed by Prof. Mamoru Yamamoto from Kyoto University. This research was supported by UTM-GUP grant number Q.J130000.2526.19H39.

REFERENCES

- [1] S. M. Buhari, M. Abdullah, A. M. Hasbi, Y. Otsuka, T. Yokoyama, M. Nishioka & T. Tsugawa, "Continuous generation and two-dimensional structure of equatorial plasma bubbles observed by high-density GPS receivers in Southeast Asia," *Journal of Geophysical Research: Space Physics*, 119(12), 10,569-510,580, 2014.
- [2] R. T. Tsunoda, "On equatorial spread F: Establishing a seeding hypothesis," *J. Geophys. Res.*, 115, A12303, 2010a.
- [3] R. T. Tsunoda & B. R. White, "On the generation and growth of backscatter plumes: 1. Wave structure in the bottomside F layer," *J. Geophys. Res.*, 86, 3610-3616, 1981.
- [4] S. Tulasi Ram, M. Yamamoto, R. T. Tsunoda, H. D. Chau, T. L. Hoang, B. Damtie, . . . T. Tsugawa, "Characteristics of large-scale wave structure observed from African and Southeast Asian longitudinal sectors," *J. Geophys. Res. A. Space Phys. Journal of Geophysical Research A: Space Physics*, 119(3), 2288-2297, 2014.
- [5] S. V. Thampi, M. Yamamoto, R. T. Tsunoda, J. Lijo & T. K. Pant, "GNU Radio Beacon Receiver (GRBR) Observations of Large-Scale Wave Structure and Equatorial Spread F (ESF)," *IEEE*, 2011.

- [6] R. T. Tsunoda, M. Yamamoto, T. Tsugawa, T. L. Hoang, S. Tulasi Ram, S. V. Thampi, H. D. Chau, and T. Nagatsuma, "On seeding, large-scale wave structure, equatorial spread F, and scintillations over Vietnam," *J. Geophys. Res. Lett.*, 38, L20102, 2011.
- [7] J. Rottger, "Wave-like structures of large-scale equatorial spread-F irregularities," *J. Atmos. Sol. Terr. Phys.*, 35, 1195–1196, 1973.
- [8] R. T. Tsunoda, "On the enigma of day-to-day variability in equatorial spread F," *Geophysical Research Letters*, 32(8), 2005.
- [9] S. V. Thampi, M. Yamamoto, R. T. Tsunoda, Y. Otsuka, T. Tsugawa, J. Uemoto & M. Ishii, "First observations of large-scale wave structure and equatorial spread F using CERTO radio beacon on the C/NOFS satellite," *Geophysical Research Letters*, 36, 18, 2009.
- [10] M. Yamamoto, "Digital beacon receiver for ionospheric TEC measurement developed with GNU Radio," *Earth Planet Sp Earth, Planets and Space*, 60(11), e21-e24, 2008.
- [11] S. M. Buhari, M. Abdullah, T. Yokoyama, Y. Otsuka, M. Nishioka, A. M. Hasbi, S. A. Bahari, ... T. Tsugawa, "Climatology of successive equatorial plasma bubbles observed by GPS ROTI over Malaysia," *Journal of Geophysical Research: Space Physics*, 122, 2, 2174–2184, 2017.
- [12] V. L. Narayanan, S. Sau, S. Gurubaran, K. Shiokawa, N. Emperumal, K. Balan, and S. Sripathi, "A statistical study of satellite traces and evolution of equatorial spread F," *Earth Planets Space*, 66, 160, 2014.
- [13] S. M. Buhari, M. Abdullah, A. M. Hasbi, S. A. Bahari, T. Yokoyama, M. Nishioka, ... "4th International Conference on Space Science and Communication, IconSpace 2015. Climatology of equatorial plasma bubble observed by MyRTKnet over the years 2008-2013," *International Conference on Space Science and Communication, Iconspace*, 101-105, 2015.
- [14] R. T. Tsunoda, "On seeding equatorial spread F: Circular gravity waves," *Geophys. Res. Lett.*, 37, L10104, 2010b.
- [15] R. T. Tsunoda, "Control of the seasonal and longitudinal occurrence of equatorial scintillations by the longitudinal gradient in integrated F region Pedersen conductivity," *J. Geophys. Res.*, 90, 447–456, 1985.
- [16] S. Tulasi Ram, P. V. S. Rama Rao, K. Niranjana, D. S. V. V. D. Prasad, R. Sridharan, C. V. Devasia, and S. Ravindhran (2006), "The role of post sunset vertical drifts at the equator in predicting the onset of VHF scintillations during high and low sunspot activity years," *Ann. Geophys.*, 24, 1609–1616, 2006.